

# Homozygous Null *TBX4* Mutations Lead to Posterior Amelia with Pelvic and Pulmonary Hypoplasia

Ariana Kariminejad,<sup>1,15,16</sup> Emmanuelle Szenker-Ravi,<sup>2,15</sup> Caroline Lekszas,<sup>3,15</sup> Homa Tajsharghi,<sup>4</sup> Ali-Reza Moslemi,<sup>5</sup> Thomas Naert,<sup>6</sup> Hong Thi Tran,<sup>6</sup> Fatemeh Ahangari,<sup>1</sup> Minoos Rajaei,<sup>7</sup> Mojila Nasser, <sup>8</sup> Thomas Haaf,<sup>3</sup> Afrooz Azad,<sup>7</sup> Andrea Superti-Furga,<sup>9</sup> Reza Maroofian,<sup>10</sup> Siavash Ghaderi-Sohi,<sup>1</sup> Hossein Najmabadi,<sup>1,11</sup> Mohammad Reza Abbaszadegan,<sup>8,12</sup> Kris Vleminckx,<sup>6</sup> Pooneh Nikuei,<sup>7,16,\*</sup> and Bruno Reversade<sup>2,13,14,16,\*</sup>

The development of hindlimbs in tetrapod species relies specifically on the transcription factor *TBX4*. In humans, heterozygous loss-of-function *TBX4* mutations cause dominant small patella syndrome (SPS) due to haploinsufficiency. Here, we characterize a striking clinical entity in four fetuses with complete posterior amelia with pelvis and pulmonary hypoplasia (PAPPA). Through exome sequencing, we find that PAPPA syndrome is caused by homozygous *TBX4* inactivating mutations during embryogenesis in humans. In two consanguineous couples, we uncover distinct germline *TBX4* coding mutations, p.Tyr113\* and p.Tyr127Asn, that segregated with SPS in heterozygous parents and with posterior amelia with pelvis and pulmonary hypoplasia syndrome (PAPPAS) in one available homozygous fetus. A complete absence of *TBX4* transcripts in this proband with biallelic p.Tyr113\* stop-gain mutations revealed nonsense-mediated decay of the endogenous mRNA. CRISPR/Cas9-mediated *TBX4* deletion in *Xenopus* embryos confirmed its restricted role during leg development. We conclude that SPS and PAPPAS are allelic diseases of *TBX4* deficiency and that *TBX4* is an essential transcription factor for organogenesis of the lungs, pelvis, and hindlimbs in humans.

Small patella syndrome (SPS, MIM: 147891), also known as ischio-pubic-patellar syndrome, ischiocoxopodopatellar syndrome with or without pulmonary arterial hypertension, coxo-podo patellar syndrome, ischiopatellar dysplasia, or Scott-Taor syndrome, is a rare autosomal dominant syndrome characterized by patellar aplasia or hypoplasia and absent, delayed, or irregular ossification of the ischiopubic junctions and/or the infra-acetabular axe-cut notches.<sup>1–5</sup> Additional features include pediatric-onset pulmonary arterial hypertension, sandal gap, short fourth and fifth rays of the feet, and occasionally pes planus.<sup>6–12</sup> In 2004, Bongers et al. identified a critical region of 5.6 cM on chromosome 17q11 via haplotype analysis in six families with SPS, and found heterozygous loss-of-function (LoF) mutations in the *T-box transcription factor 4* (*TBX4*) gene (MIM: 601719) to be responsible for this syndrome.<sup>13</sup> Recently, the occurrence of rare coding *TBX4* variants with putative hypomorphic non-coding mutations in one of its lung enhancers has been recognized as a cause of pediatric pulmonary hypertension and lethal lung developmental disease, which is associated

with congenital heart disease, foot anomalies, and developmental disability.<sup>14–17</sup>

*T-box* genes are a family of evolutionary-conserved transcription factors characterized by a shared DNA-binding domain. They have restricted spatio-temporal patterns of expression during embryogenesis, and play distinct roles during organogenesis as documented by genetic studies performed in animal models and humans.<sup>18–23</sup> Studies in animal models have revealed the importance of *Tbx4* in hindlimb development.<sup>24–26</sup> The misexpression of a dominant-negative *Tbx4* construct causes legless chickens with deformed and hypoplastic pelvis and absent pubis.<sup>26,27</sup> In mice, a homozygous *Tbx4*-null allele entirely abrogates hindlimb development while forelimbs remain unaffected.<sup>24</sup> *TBX4* is a transcriptional activator of the short stature homeodomain transcription factor 2 (*SHOX2*) during murine fore- and hindlimb development, and is itself regulated by *SHOX2* specifically in the forelimb bud, possibly via a positive feedback loop.<sup>28</sup>

Interestingly, autosomal dominant mutations in the paralogous gene *TBX3* are responsible for Ulnar-Mammary

<sup>1</sup>Kariminejad-Najmabadi Pathology and Genetics Center, Tehran 14665, Iran; <sup>2</sup>Institute of Medical Biology, Agency for Science, Technology, and Research, 8A Biomedical Grove, Singapore 138648, Republic of Singapore; <sup>3</sup>Institute of Human Genetics, Julius-Maximilians-Universität, 97074 Würzburg, Germany; <sup>4</sup>School of Health Sciences, Division Biomedicine, University of Skövde, 54128 Skövde, Sweden; <sup>5</sup>Institute of Biomedicine, Sahlgrenska University Hospital, Gothenburg University, 41390 Gothenburg, Sweden; <sup>6</sup>Department of Biomedical Molecular Biology, Ghent University, B-9052 Ghent, Belgium; <sup>7</sup>Fertility and Infertility Research Center, Hormozgan University of Medical Sciences, Bandar Abbas 7919915519, Iran; <sup>8</sup>Pardis Clinical and Genetics Laboratory, Mashhad 9177948974, Iran; <sup>9</sup>Division of Genetic Medicine, Lausanne University Hospital (CHUV), University of Lausanne, 1011 Lausanne, Switzerland; <sup>10</sup>Molecular and Clinical Sciences Institute, St. George's University of London, Cranmer Terrace, London SW17 0RE, UK; <sup>11</sup>Genetics Research Center, University of Social Welfare and Rehabilitation Sciences, Tehran 1985713834, Iran; <sup>12</sup>Division of Human Genetics, Immunology Research Center, Avicenna Research Institute, Mashhad University of Medical Sciences, Mashhad 15731, Iran; <sup>13</sup>Institute of Molecular and Cell Biology, Agency for Science, Technology, and Research, 61 Biopolis Drive, Singapore 138673, Republic of Singapore; <sup>14</sup>Department of Medical Genetics, Koç University, School of Medicine, 34010 Topkapı, Istanbul, Turkey

<sup>15</sup>These authors contributed equally to this work

<sup>16</sup>These authors contributed equally to this work

\*Correspondence: poonehnikuei@gmail.com (P.N.), bruno@reversade.com (B.R.)

<https://doi.org/10.1016/j.ajhg.2019.10.013>

© 2019 American Society of Human Genetics.



syndrome (UMS, MIM: 181450), which is predominantly characterized by posterior forelimb deficiencies or duplications, with rare involvement of the hindlimbs, and apocrine and mammary gland hypoplasia or dysfunction, with absent or abnormal nipples.<sup>29</sup> In mouse, *Tbx3* expression is observed in both forelimbs and hindlimbs,<sup>30</sup> and homozygous mutant embryos exhibit both forelimb and hindlimb abnormalities.<sup>31</sup> These embryos also present with a deficiency of mammary gland induction.<sup>31</sup> In contrast, autosomal dominant mutations in *TBX5* lead to Holt-Oram syndrome (HOS, MIM: 142900), which is characterized by anterior upper limb amelia and cardiac abnormalities.<sup>32,33</sup> *Tbx5* is specifically expressed in the heart and developing forelimb buds, and its inactivation in mice phenocopies HOS.<sup>34,35</sup> *Tbx4* and *Tbx5* are thus crucial in the specification of hindlimbs and forelimbs, respectively,<sup>25,36</sup> and are both upstream regulators of FGF10 and RSPO2, which drive the outgrowth of all four limb buds.<sup>26,27,37</sup>

In this study, we identify two consanguineous families from Iran segregating a recessively inherited lethal embryonic syndrome. In four affected fetuses displaying absent hindlimbs with pelvis and pulmonary hypoplasia, we identified via exome sequencing two distinct germline homozygous LoF mutations in *TBX4* as the cause of this hitherto undescribed disease. We propose to name this clinical entity posterior amelia with pelvis and pulmonary hypoplasia syndrome (PAPPAS). Functional tests in *Xenopus tropicalis* confirmed that *TBX4* is needed for posterior limb and pelvis development but not for forelimb development. Because the heterozygous parents of these two families also presented with skeletal features consistent with SPS, we conclude that these two Mendelian diseases are allelic. We propose that the heterozygous loss of *TBX4* is incompletely dominant while its recessive form in PAPPAS demonstrates its essentiality for hindlimb, pelvis, and lung development in humans.

The fetus F1-IV:5 is the result of a fifth pregnancy of related Iranian parents (Figure 1A). The first pregnancy resulted in a stillborn fetus born at term. The genitalia were ambiguous and lower limbs were not formed. Ultrasound examination, X-rays, or pictures were not taken from this first fetus. The second and third pregnancies resulted in healthy boys now aged 14 and 10 years. The fourth pregnancy was followed by ultrasound examination, and the absence of lower limbs was noted at 15 weeks of gestation, and elective abortion was performed at 16 weeks of pregnancy. Autopsy examination was not performed. The fifth pregnancy was controlled with ultrasound, and the absence of lower limbs and severe hypoplasia of pelvic bones was detected at 15 weeks of pregnancy, elective abortion was performed at 16 weeks of pregnancy, and the fetus was sent for autopsy examination. In this and previous pregnancies, the mother did not have any history of drug ingestion or exposure to known teratogens. Gross findings of F1-IV:5 included completely absent lower limbs, anal atresia, ambiguous

genitalia, rectoperineal fistula, muscular hypoplasia of the upper limbs, atresia of external auditory canals, hypoplastic lungs, and pulmonary segmentation defect (Figure 1B). Measurements were as follows: crown rump (120 mm, -0.09 SD), head circumference (110 mm, -1.08 SD), and weight (77 grams, -1.08 SD). The heart, liver, gallbladder, stomach, duodenum, jejunum, ileum, and colon were normal. The rectum ended in a blind pouch which was connected to the perineum with a narrow fistula tract. Microscopic findings included severe hypoplasia of the lungs with no apparent differentiation, and mild pyelocaliceal dilatation. X-ray examination showed complete absence of lower limbs, absent pelvic bones, and hypoplastic sacrum (Figure 1B).

The fetus F2-IV:3 in Family 2 is the result of a third pregnancy of first-cousin Iranian parents (Figure 1A). The first pregnancy resulted in a healthy girl, and the second pregnancy resulted in a miscarriage. For the third pregnancy, sonography at gestational week 16 + 3 showed a living fetus with reduced movements, who demonstrated bilateral absence of the posterior extremities (femur, tibia, and fibula). The parents decided to abort the pregnancy and no photography or detailed autopsy of the fetus could be performed.

Whole-exome sequencing (WES) in fetus VI:5 of Family 1 uncovered a private homozygous nonsense variant (c.339T>A) in exon 4 of *TBX4* (RefSeq accession number NM\_001321120.1) that is predicted to result in a stop codon and premature truncation at codon 113 (p.Tyr113\*) (Figure 1C). Co-segregation study in available family members revealed that both parents were heterozygous and that the two unaffected siblings were non-carriers for this rare *TBX4* variant (Figure S1A). Because the c.339T>A variant was predicted to cause a premature stop codon probably leading to nonsense-mediated decay (NMD) of the endogenous mRNA, an RT-PCR analysis was carried out on cDNA extracted from forelimb tissue. This analysis showed no detectable expression levels of endogenous *TBX4* transcripts in the F1-IV:5 fetus, while expression was found in forelimb tissue from a control fetus of the same age (Figure 1D). These data confirm that the c.339T>A *TBX4* variant leads to complete destabilization of the endogenous transcript by NMD. This may therefore constitute the first protein-null or knockout *TBX4* allele in humans.

Exome capture in the parents of Family 2 revealed a single-nucleotide-variant (c.379T>A) in exon 4 of *TBX4* (RefSeq accession number NM\_001321120.1) that results in a heterozygous missense mutation p.Tyr127Asn in the evolutionary conserved DNA-binding domain of *TBX4* (Figure 1C). This rare *TBX4* c.379T>A (p.Tyr127Asn) variant was absent from all available population databases including ExAc, and also absent from our in-house database of 10,000 exomes. It has a combined annotation-dependent depletion (CADD,<sup>38</sup>) score of 29.8, which predicts it to be highly pathogenic, as is also suggested by other *in silico* predictors such as MutationTaster and

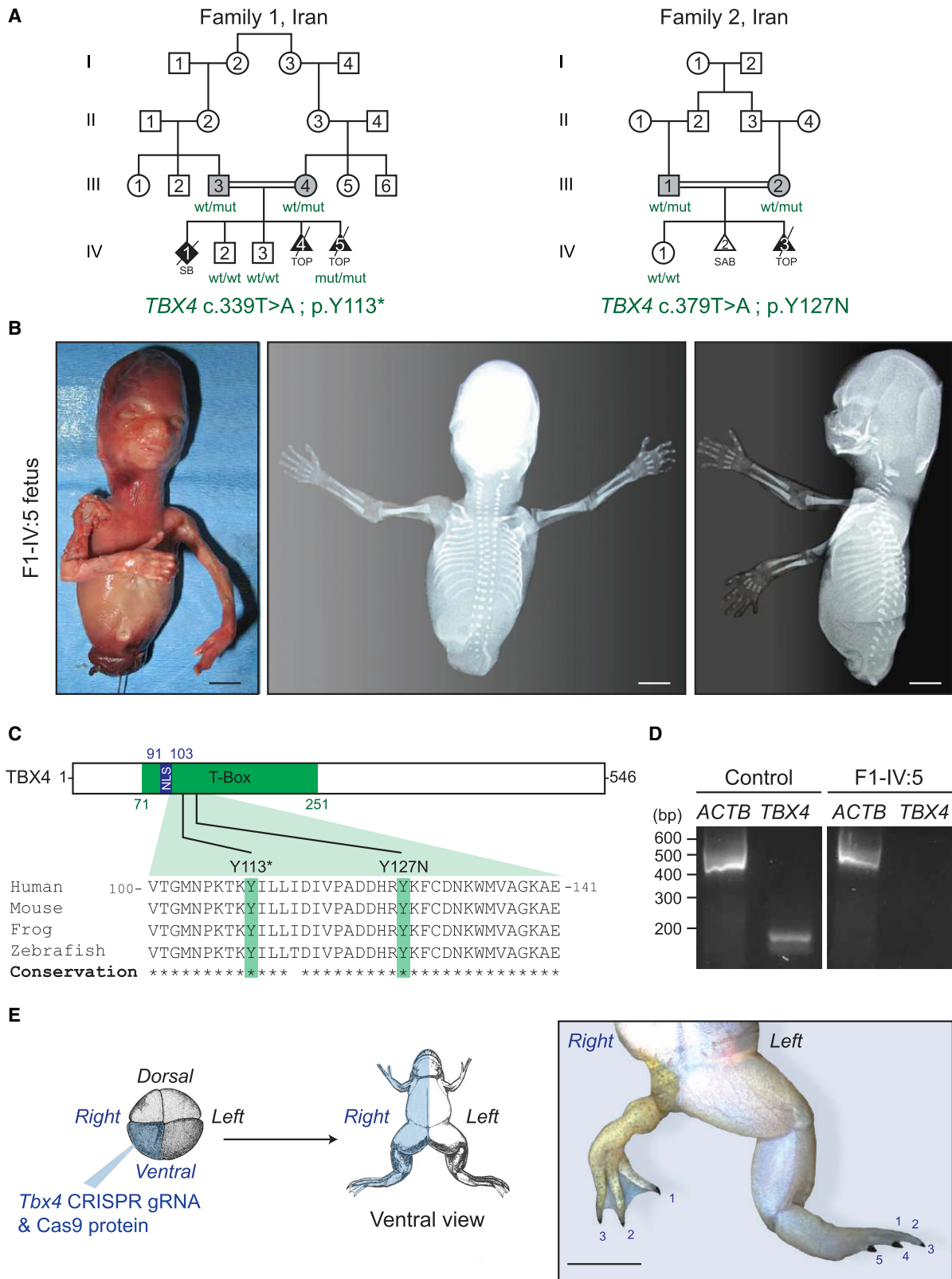


**Figure 1. PAPPAS Is Caused by *TBX4* Recessive Loss-of-Function Mutations**

(A) Pedigrees of two consanguineous Iranian families segregating small patella syndrome in heterozygous *TBX4* individuals (gray) and posterior amelia with pelvis and pulmonary hypoplasia syndrome (PAPPAS) in homozygous fetuses (black). The identified mutation and the genotype of available family members are indicated in green. Squares, circles, diamonds, and triangles denote males, females, unknown gender individuals, and fetuses, respectively. Open symbols are used for unaffected family members, and deceased individuals

(legend continued on next page)

SIFT. The heterozygosity of both parents for this variant is consistent with their SPS phenotype, and co-segregation study confirmed that the unaffected sister was wild-type (Figure S1B). Unfortunately, DNA from the affected fetus was not available.

In order to further document the causal link between *TBX4* deficiency and hindlimb development defects, we injected *tbx4* gRNA1 with Cas9 protein unilaterally in one ventral blastomere of four-cell-stage *Xenopus tropicalis* embryos (Figure 1E). Successful genome editing was validated via targeted deep sequencing (Table S1). Across two experimental repeats, 10% (n = 31) and 6.66% (n = 30), respectively, of the resulting F0 mosaic tadpoles (crispants) manifested striking unilateral hindlimb defects (Figure 1E), but forelimb anomalies were never observed. The most strongly affected animals had a severely underdeveloped hindlimb with a reduced number of toes that still carried claws, a typical characteristic of hindlimbs in *Xenopus* species. Strikingly, the affected limbs were completely covered with pigmented skin, which is normally present only on the dorsal side, suggesting that *Tbx4* inactivation may lead to dorsalization of the affected hindlimb. The less severely affected animals presented with normal forelimbs on the injected side, while the hindlimbs were smaller and not used for swimming. Alizarin red and alcian blue staining of these animals showed a shorter femur and dislocated joints, both at the hip and the knee (Figure S2). In order to confirm the hindlimb phenotype with a second gRNA and to completely recapitulate hindlimb amelia as seen in patients, we also injected *tbx4* gRNA2 pre-complexed with Cas9 protein unilaterally in two-cell-stage *Xenopus tropicalis* embryos (data not shown). With this gRNA, almost universal genome editing was seen on the injected side (Table S1), and all animals manifested a very apparent growth delay and died before limb formation around 35 days post-injection, potentially due to lung defects. Unfortunately, this precluded the identification of potential hindlimb amelia. Together, these *in vivo* functional tests confirm the importance of *TBX4* during embryonic development in vertebrates, including a role for proper hindlimb morphogenesis.

Heterozygous *TBX4* mutations are known to lead to dominant SPS.<sup>13</sup> We thus examined the parents of the PAPPAS fetuses, who are obligate heterozygous carriers of the identified germline *TBX4* mutations. X-ray examination showed the classical findings of SPS in the parents of Family 1 (III:3 and III:4), including patellar hypoplasia,

absent or delayed or irregular ossification of the ischiopubic junctions and/or the infra-acetabular axe-cut, and short fourth and fifth rays of the feet (Figure 2A). The two healthy sons (IV:2 and IV:3), who are wild-type for the variant, do not show any of the X-ray findings associated with SPS. For Family 2, X-ray examination of the parents (III:1 and III:2) also revealed phenotypes consistent with SPS, which included patellar hypoplasia, thin ischial bones, and sandal gap between the first and second toes (Figure 2B). Abnormal ischio-pubic junction and short fourth and fifth rays of the feet were also observed in the mother (Figure 2B). Altogether, these findings confirm the pathogenicity of these two germline *TBX4* LoF variants. We therefore conclude that while heterozygous *TBX4* mutations are responsible for SPS, when homozygously inherited, the same alleles lead to lethal PAPPAS characterized by caudal regression with complete posterior amelia and pelvic aplasia.

Inactivation of *Tbx4* has different effects depending on the timing of limb development. When it is deleted before limb bud formation, the hindlimbs fail to develop altogether, but if it is inactivated during limb outgrowth, a dramatic loss of proximal skeletal elements and a mild loss of distal skeletal elements are seen.<sup>39</sup> Our results in *Xenopus* support this as the least affected frogs showed more severe proximal than distal hindlimb anomalies. Our observation that pigmented skin, which is normally restricted to the dorsal side of the animal, was covering the affected limbs of *TBX4* crispant froglets could indicate that *TBX4* plays a role in specifying, or maintaining, ventral identity in developing hindlimbs. Alternatively, this may be interpreted as a failure of hindlimbs to properly articulate at the levels of the pelvis so that they instead point backwards, a phenomenon seen in conditional *Tbx4* mutant mice.<sup>39</sup>

All of the affected fetuses with homozygous *Tbx4* mutations present with complete absence of lower limbs, absent pelvic bones, and hypoplastic sacrum. These phenotypes were to be anticipated based on animal models of *TBX4* inactivation. Loss of *TBX4* in mice cancels hindlimb development while forelimbs remain unaffected,<sup>24</sup> and dominant-negative *Tbx4* overexpression leads to chickens bereft of legs, with deformed and hypoplastic pelvis and absent pubis.<sup>26,27</sup> Of note, *TBX4* in humans does not seem to be essential for umbilical cord formation since *TBX4* knockout fetuses can reach full term (F1-IV:1), while mice

---

are indicated by a diagonal slash through the symbol. Wt, wildtype; mut, mutant; SB, stillbirth; TOP, termination of pregnancy; SAB, spontaneous abortion.

(B) Photographs and X-rays of affected fetus IV:5 in Family 1 with a germline homozygous p.Y113X *TBX4* mutation. Scale bars: 1 cm.

(C) Phylogenetic alignment performed with Clustal O, and position of germline recessive *TBX4* mutations in the conserved T-box domain of the transcription factor *TBX4*. NLS, nuclear localization signal.

(D) *TBX4* and *ACTB* RT-PCR analysis on cDNA extracted from forelimb tissues of a control and the F1-IV:5 fetuses indicating complete absence of the endogenous *TBX4* transcript in the mutant fetus. bp, base pairs.

(E) *Xenopus tropicalis* crispants show severe hindlimb dysplasia after injection of *tbx4*\_gRNA1 pre-complexed with Cas9 protein in one ventral cell of a four-cell-stage embryo (blue), thereby targeting the ventral lineage unilaterally, i.e. primarily the lateral plate mesoderm and the epidermis. A representative post-metamorphic animal (NF stage 66) injected on the right side is shown; the number of toes is indicated. Scale bar: 0.5 cm, ventral view.



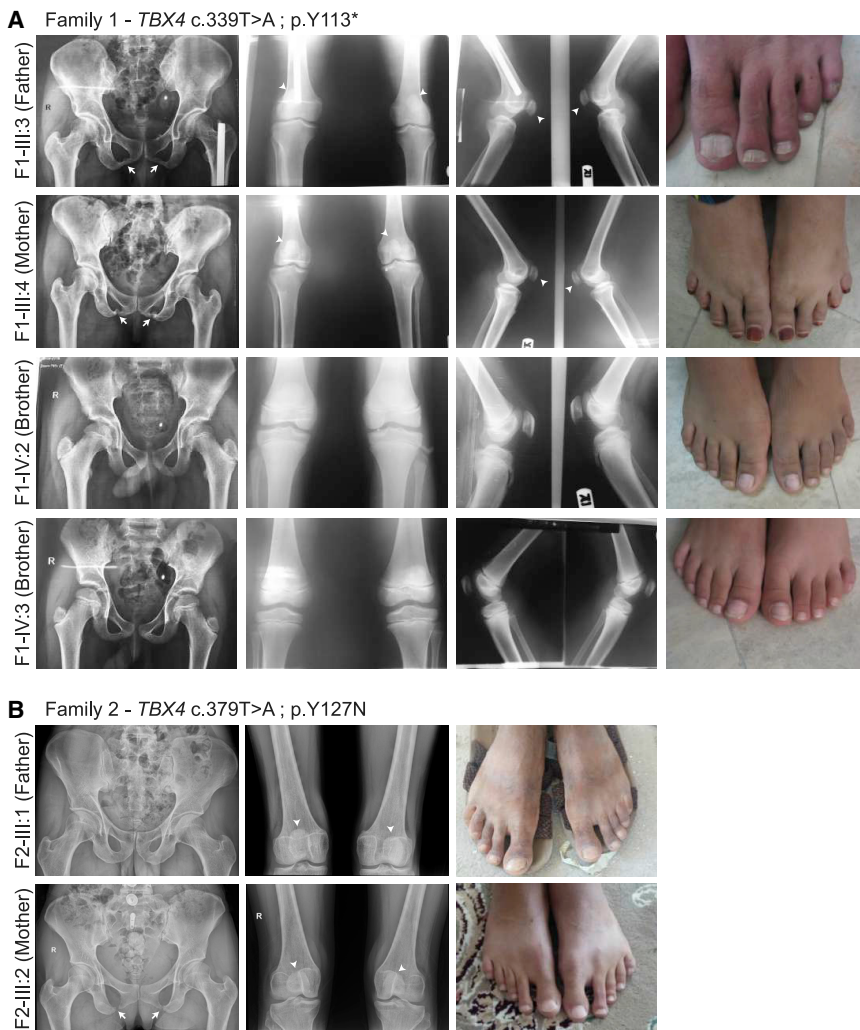


**Figure 2. The Heterozygous *TBX4* Parents Present with SPS**

X-ray and photographs of the indicated family members in Family 1 (A) and Family 2 (B). White arrows point to abnormal ischio-pubic junction, and arrowheads point to hypoplastic patellae in both heterozygous parents of the two families. Note the short fourth and fifth rays in the feet of both parents in Family 1 and the mother in Family 2, and the wide gap between the first and second toes in both parents of Family 2.

hypoplasia, and alveolar growth abnormality.<sup>14–17,41</sup> Of note, the F1-IV:5 fetus also showed atresia of external auditory canal. We are not aware of previous reports of abnormalities in external ear development in association with *TBX4* variants or CNVs in humans or other organisms, but there are reports of deletions and/or duplications of the region containing the *TBX4* gene associated with hearing loss and abnormal auricles.<sup>42–44</sup>

From an evolutionary perspective, *TBX4* is not essential in lower vertebrate species. The naturally occurring *Tbx4* mutant zebrafish known as “pelvic fin-loss” is fertile and shows a viable phenotype with absent pelvic fins, which are analogous to posterior limbs in tetrapod species.<sup>45</sup> Notably, *Tbx4* is entirely lost in the seahorse

*Hippocampus comes* who has only retained *Tbx5* for the specification of pectoral fins, which are analogous to forelimbs in tetrapods.<sup>46</sup>

Taken together, our clinical, genetic, molecular, and embryological studies define a heretofore unknown monogenic syndrome caused by homozygous null *TBX4* mutations. This embryonic lethal condition, which we propose to name PAPPAS, is allelic to SPS. Together, these Mendelian conditions delineate a spectrum of severity driven by either monoallelic or biallelic *TBX4* deficiency in humans.

## Online Materials and Methods

### Editorial Policies and Ethical Considerations

This study was approved in Iran by the ethics committees of the Kariminejad-Najmabadi Pathology and Genetics Center for Family 1, and of Mashhad University of Medical Sciences and Pardis Genetic Laboratory for Family 2. The parents of both families provided written informed consent to participate in this study and to publish their family pedigrees and clinical data. All clinical investigations were conducted according to the principles expressed in the Declaration of Helsinki.

lacking *Tbx4* die at mid-gestation (E10.5) due to defects in the vascularization and fusion of the allantois.<sup>24</sup> However, the fetus F1-IV:5 showed additional features including muscular hypoplasia of upper limbs, atresia of external auditory canals, and hypoplastic lungs and pulmonary segmentation defect. The short stature homeodomain transcription factor *SHOX2* is a key player during limb development; its loss in mouse is associated with altered muscular development and innervation defects of the proximal forelimbs.<sup>40</sup> Interestingly, Glaser et al. showed that *Tbx4*<sup>-/-</sup> mouse embryos present with a reduced expression of *Shox2* in forelimbs and hindlimbs, and suggested that regulation of *Tbx4* by *SHOX2* may contribute to the development of muscular and skeletal elements in the developing mammalian forelimb.<sup>28</sup> Therefore, the hypoplasia of upper limbs observed in the F1-IV:5 fetus is in line with the suggested role of *TBX4* in forelimb muscular development. This fetus also had hypoplastic lungs and pulmonary segmentation defects. The role of *TBX4* on lung development has recently been studied in humans. Complex non-coding variants in the lung enhancer of *TBX4* in conjunction with coding mutations in *TBX4* cause severe lung abnormalities such as acinar dysplasia, congenital alveolar dysplasia, pulmonary

## Genetic Analysis

WES was performed on gDNA of aborted fetus IV:5 of Family 1 after obtaining written informed consent. Exome capture was performed using the Agilent SureSelect Human All Exon V6 Kit with 150-bp paired-end read sequences generated on a HiSeq4000; 2× 100bp. Sequences were aligned to hg19, and variants were identified through the GATK pipeline. Variations were annotated with ANNOVAR. Identified variants were checked against public databases dbSNP ver.149, Exome Variant Server, ExAC, and Iranome. Co-segregation of the variant was examined in the available family members via bidirectional Sanger sequencing (Figure S1).

Exome capture in the parents of Family 2 was conducted following the Illumina Nextera Rapid Capture Enrichment library preparation protocol using 50 ng of genomic DNA. Paired-end sequencing of the library was performed using a NextSeq500 desktop sequencer (Illumina) with a v2 reagent kit (Illumina). The generated sequences were demultiplexed and mapped to the human genome reference (NCBI build37/hg19 version) with Burrows-Wheeler Aligner. Variant calling and analysis was conducted using GensearchNGS software (PhenoSystems SA). Variants with a coverage of  $\leq 20$ , a Phred-scaled quality of  $\leq 15$ , a frequency of  $\leq 20$ , and a MAF of  $\geq 1\%$  were filtered out. Alamut® Visual (Interactive Biosoftware), with its incorporated prediction tools like SIFT, MutationTaster, and PolyPhen-2, was used for variant prioritization. Co-segregation of the variant was examined in the available family members via bidirectional Sanger sequencing.

## Transcript Analysis

Total RNA was extracted from forelimb tissue of affected fetus of Family 1 (IV:5) through the use of the Total RNA Isolation System (Promega). Synthesis of first-strand complementary DNA (cDNA) was performed using the iScript cDNA Synthesis kit (Bio-Rad Laboratories), according to the manufacturer's instructions using 0.4  $\mu\text{g}$  total RNA. To analyze the impact of the c.339T>A variant in transcript expression of *TBX4* in the affected fetus of Family 1, reverse-transcriptase (RT)-PCR was performed on cDNA extracted from forelimb tissue with primer pairs covering part of exon 1 through exon 4 generating an amplicon of 181 bp (forward primer 5'-CAG ACC ATC GAG AAC ATC AAG-3' and reverse primer 5'-GCA GGG ACA ATG TCA ATC AG-3'). The 496 bp amplification of the cDNA encoding beta-actin (*ACTB*) served as an endogenous quality control (forward primer 5'-GGC ATC CTC ACC CTG AAG TA-3' and reverse primer 5'-CCA TCT CTT GCT CGA AGT CC-3').

## Generation of *Xenopus tropicalis* Mosaic Mutants by CRISPR/Cas9

All experiments on *Xenopus tropicalis* were executed in accordance with the guidelines and regulations of Ghent University, faculty of Sciences, Belgium. Approval was obtained by the ethical committee of Ghent University, faculty of Sciences (permit number EC2017-093). In brief,

two guide RNA targeting *Tbx4* were designed with CRISPR-Scan, generated as previously described,<sup>47,48</sup> and yield was quantified by Qubit BR RNA assay (ThermoFischer Scientific). Embryos were injected either in one ventral blastomere at the four-cell stage (*tbx4*\_gRNA1) or unilaterally in a two-cell-stage embryo (*tbx4*\_gRNA2) with 47 pg of *tbx4* gRNA and 900 pg of NLS-Cas9-NLS (VIB/UGent Protein Service Facility), and adult animals were analyzed at Nieuwkoop-Faber stage 66. The gRNA and PCR primer sequences used are as follows: *tbx4*\_gRNA1, gRNA target 5'-GGT GTT GAG TGG CAA GTC CT-3', forward primer 5'-AGG CAA AGA CTG GTA TCA A-3', reverse primer 5'-ACC TGG GTA GAA TGA GAA-3'; *tbx4*\_gRNA2, gRNA target 5'-TGA TGA CAG TGA CCT CCG TGT GG-3', forward primer 5'-ATA TTT ACC CAC ACC AGC C-3', reverse primer 5'-TTT CCA ATG CCA GTA TCC AC-3'. For quantitative analysis of genome editing, nine embryos per injected clutch were pooled and lysed overnight in lysis buffer (50 mM Tris pH 8.8, 1 mM EDTA, 0.5% Tween-20, 200  $\mu\text{g}/\text{ml}$  proteinase K) at 55°C.

Genotyping PCRs were performed with the respective primer pairs. Targeted deep sequencing of amplicons was performed as previously described and analyzed by the BATCH-GE software package.<sup>49</sup> Indel frequency data and sequence variants for all targeted deep sequencing are shown in Table S1. Note that the maximum expected efficiency is 25% for gRNA1 and 50% for gRNA2 because the injections were performed in one cell out of four or two cells, respectively. For staining of the skeletons of the mutant animals, premetamorphic tadpoles and post-metamorphic froglets were euthanized using a 0.05% benzocaine solution. Animals were fully eviscerated and skinned and eyes were removed. Whole mount alcian blue/alizarin red stainings were performed as follows: 95% EtOH (4 days, change after 24h), 100% acetone (48 h), 0.15% alcian blue 8G× (Sigma-Aldrich A3157) in 76% EtOH/20% glacial acetic acid/4% H<sub>2</sub>O (24 h), 70% EtOH (24 h), 95% EtOH (12 h), 1% KOH (6 h), 0.05% alizarin red S (Sigma-Aldrich A5533) in 1% KOH (48 h), 1% KOH (48 h). Imaging was performed with a Leica MZ FLIII stereomicroscope/Leica DC300F camera.

## Accession Numbers

The WES data for Family 1 and Family 2 have been deposited in the NCBI Sequence Read Archive (SRA) database under accession numbers PRJNA578898 and PRJNA578086, respectively.

## Supplemental Data

Supplemental Data can be found online at <https://doi.org/10.1016/j.ajhg.2019.10.013>.

## Acknowledgements

We thank members of both families who provided samples and clinical information for this study. H.T. was supported by grants from the European Union's Seventh Framework Programme for

research, technological development, and demonstration under grant agreement no. 608473 and the Swedish Research Council. E.S.-R. is supported by a National Medical Research Council Open Fund—Young Individual Research Grant (OF-YIRG, #OFYIRG18May-0053). T.N. is funded by Kom op tegen Kanker (Stand up to Cancer), the Flemish cancer society. B.R. is a fellow of the Branco Weiss Foundation, an A\*STAR Investigator, a National Research Foundation and Amsterdam Academic Alliance (AAA) fellow, and an European Molecular Biology Organization (EMBO) Young Investigator. This work was partly funded by a Strategic Positioning Fund on Genetic Orphan Diseases from A\*STAR, Singapore. The funders had no role in the design of the study and collection, analysis, decision to publish, interpretation of data, or preparation of the manuscript.

## Declaration of Interests

The authors declare no competing interests.

Received: July 18, 2019

Accepted: October 25, 2019

Published: November 21, 2019

## Web Resources

1000 Genomes Project Database, <http://browser.1000genomes.org/index.html>

CRISPRScan, <https://www.crisprscan.org>

Exome Aggregation Consortium (ExAC), <http://exac.broadinstitute.org>

Exome Variant Server from NHLBI Exome Sequencing Project (ESP), <https://evs.gs.washington.edu/EVS/>

Genome Aggregation Database (GnomAD), <http://gnomad.broadinstitute.org/>

Greater Middle East (GME) Variome web, <http://igm.ucsd.edu/gme/index.php>

NCBI dbSNP, <https://www.ncbi.nlm.nih.gov/SNP/>

Online Mendelian Inheritance in Man (OMIM), <https://www.omim.org>

Iranome database, <http://www.iranome.com>

## References

1. Vaněk, J. (1981). [Ischiopatellar dysplasia (Scott and Taor's syndrome of the small patella)]. *RoFo Fortschr. Geb. Rontgenstr. Nuklearmed.* 135, 354–356.
2. Morin, P., Vielpeau, C., Fournier, L., and Denizet, D. (1985). [The coxopodopatellar syndrome]. *J. Radiol.* 66, 441–446.
3. Scott, J.E., and Taor, W.S. (1979). The “small patella” syndrome. *J. Bone Joint Surg. Br.* 61-B, 172–175.
4. Dellestable, F., Péré, P., Blum, A., Régent, D., and Gaucher, A. (1996). The ‘small-patella’ syndrome. Hereditary osteodysplasia of the knee, pelvis and foot. *J. Bone Joint Surg. Br.* 78, 63–65.
5. Poznanski, A.K. (1997). Comments on the ischio-pubic-patellar syndrome. *Pediatr. Radiol.* 27, 428–429.
6. Sandhaus, Y.S., Ben-Ami, T., Chechick, A., and Goodman, R.M. (1987). A new patella syndrome. *Clin. Genet.* 31, 143–147.
7. Kozłowski, K., and Nelson, J. (1995). Small patella syndrome. *Am. J. Med. Genet.* 57, 558–561.
8. Azouz, E.M., and Kozłowski, K. (1997). Small patella syndrome: a bone dysplasia to recognize and differentiate from the nail-patella syndrome. *Pediatr. Radiol.* 27, 432–435.
9. Habboub, H.K., and Thneibat, W.A. (1997). Ischio-pubic-patellar hypoplasia: is it a new syndrome? *Pediatr. Radiol.* 27, 430–431.
10. Bongers, E.M., Van Bokhoven, H., Van Thienen, M.N., Kooyman, M.A., Van Beersum, S.E., Boetes, C., Knoers, N.V., and Hamel, B.C. (2001). The small patella syndrome: description of five cases from three families and examination of possible allelism with familial patella aplasia-hypoplasia and nail-patella syndrome. *J. Med. Genet.* 38, 209–214.
11. Levy, M., Eyries, M., Szezepanski, I., Ladouceur, M., Nadaud, S., Bonnet, D., and Soubrier, F. (2016). Genetic analyses in a cohort of children with pulmonary hypertension. *Eur. Respir. J.* 48, 1118–1126.
12. Kerstjens-Frederikse, W.S., Bongers, E.M.H.F., Roofthoof, M.T.R., Leter, E.M., Douwes, J.M., Van Dijk, A., Vonk-Noordegraaf, A., Dijk-Bos, K.K., Hoefsloot, L.H., Hoendermis, E.S., et al. (2013). TBX4 mutations (small patella syndrome) are associated with childhood-onset pulmonary arterial hypertension. *J. Med. Genet.* 50, 500–506.
13. Bongers, E.M.H.F., Duijf, P.H.G., van Beersum, S.E.M., Schoots, J., Van Kampen, A., Burckhardt, A., Hamel, B.C.J., Losan, F., Hoefsloot, L.H., Yntema, H.G., et al. (2004). Mutations in the human TBX4 gene cause small patella syndrome. *Am. J. Hum. Genet.* 74, 1239–1248.
14. Galambos, C., Mullen, M.P., Shieh, J.T., Schwerk, N., Kieft, M.J., Ullmann, N., Boldrini, R., Stucin-Gantar, I., Haass, C., Bansal, M., et al. (2019). Phenotype characterisation of TBX4 mutation and deletion carriers with neonatal and paediatric pulmonary hypertension. *Eur. Respir. J.* 54, 1801965.
15. Karolak, J.A., Szafranski, P., Kilner, D., Patel, C., Scurry, B., Kinning, E., Chandler, K., Jhangiani, S.N., Coban Akdemir, Z.H., Lupski, J.R., et al. (2019). Heterozygous CTNBN1 and TBX4 variants in a patient with abnormal lung growth, pulmonary hypertension, microcephaly, and spasticity. *Clin. Genet.* 96, 366–370.
16. Suhrie, K., Pajor, N.M., Ahlfeld, S.K., Dawson, D.B., Dufendach, K.R., Kitzmiller, J.A., Leino, D., Lombardo, R.C., Smolarek, T.A., Rathbun, P.A., et al. (2019). Neonatal lung disease associated with TBX4 mutations. *J. Pediatr.* 206, 286–292.e1.
17. Szafranski, P., Coban-Akdemir, Z.H., Rupps, R., Grazioli, S., Wensley, D., Jhangiani, S.N., Popek, E., Lee, A.F., Lupski, J.R., Boerkoel, C.F., and Stankiewicz, P. (2016). Phenotypic expansion of TBX4 mutations to include acinar dysplasia of the lungs. *Am. J. Med. Genet. A.* 170, 2440–2444.
18. Herrmann, B.G., and Kispert, A. (1994). The T genes in embryogenesis. *Trends Genet.* 10, 280–286.
19. Smith, J. (1999). T-box genes: What they do and how they do it. *Trends Genet.* 15, 154–158.
20. Papaioannou, V.E., and Silver, L.M. (1998). The T-box gene family. *BioEssays* 20, 9–19.
21. Papaioannou, V.E. (2001). T-box genes in development: from hydra to humans. *Int. Rev. Cytol.* 207, 1–70.
22. Haworth, K., Putt, W., Cattanaach, B., Breen, M., Binns, M., Lingaas, F., and Edwards, Y.H. (2001). Canine homolog of the T-box transcription factor T; failure of the protein to bind to its DNA target leads to a short-tail phenotype. *Mamm. Genome* 12, 212–218.



23. Ghosh, T.K., Brook, J.D., and Wilsdon, A. (2017). T-box genes in human development and disease. *Curr. Top. Dev. Biol.* *122*, 383–415.
24. Naiche, L.A., and Papaioannou, V.E. (2003). Loss of Tbx4 blocks hind limb development and affects vascularization and fusion of the allantois. *Development* *130*, 2681–2693.
25. Rodriguez-Esteban, C., Tsukui, T., Yonei, S., Magallon, J., Tamura, K., and Izpisua Belmonte, J.C. (1999). The T-box genes Tbx4 and Tbx5 regulate limb outgrowth and identity. *Nature* *398*, 814–818.
26. Takeuchi, J.K., Koshiba-Takeuchi, K., Suzuki, T., Kamimura, M., Ogura, K., and Ogura, T. (2003). Tbx5 and Tbx4 trigger limb initiation through activation of the Wnt/Fgf signaling cascade. *Development* *130*, 2729–2739.
27. Agarwal, P., Wylie, J.N., Galceran, J., Arkhitko, O., Li, C., Deng, C., Grosschedl, R., and Bruneau, B.G. (2003). Tbx5 is essential for forelimb bud initiation following patterning of the limb field in the mouse embryo. *Development* *130*, 623–633.
28. Glaser, A., Arora, R., Hoffmann, S., Li, L., Gretz, N., Papaioannou, V.E., and Rappold, G.A. (2014). Tbx4 interacts with the short stature homeobox gene Shox2 in limb development. *Dev. Dyn.* *243*, 629–639.
29. Bamshad, M., Lin, R.C., Law, D.J., Watkins, W.C., Krakowiak, P.A., Moore, M.E., Franceschini, P., Lala, R., Holmes, L.B., Gebuhr, T.C., et al. (1997). Mutations in human TBX3 alter limb, apocrine and genital development in ulnar-mammary syndrome. *Nat. Genet.* *16*, 311–315.
30. Gibson-Brown, J.J., Agulnik, S.I., Chapman, D.L., Alexiou, M., Garvey, N., Silver, L.M., and Papaioannou, V.E. (1996). Evidence of a role for T-box genes in the evolution of limb morphogenesis and the specification of forelimb/hind limb identity. *Mech. Dev.* *56*, 93–101.
31. Davenport, T.G., Jerome-Majewska, L.A., and Papaioannou, V.E. (2003). Mammary gland, limb and yolk sac defects in mice lacking Tbx3, the gene mutated in human ulnar mammary syndrome. *Development* *130*, 2263–2273.
32. Basson, C.T., Bachinsky, D.R., Lin, R.C., Levi, T., Elkins, J.A., Soultz, J., Grayzel, D., Kroumpouzou, E., Traill, T.A., Leblanc-Straceski, J., et al. (1997). Mutations in human TBX5 [corrected] cause limb and cardiac malformation in Holt-Oram syndrome. *Nat. Genet.* *15*, 30–35.
33. Li, Q.Y., Newbury-Ecob, R.A., Terrett, J.A., Wilson, D.I., Curtis, A.R., Yi, C.H., Gebuhr, T., Bullen, P.J., Robson, S.C., Strachan, T., et al. (1997). Holt-Oram syndrome is caused by mutations in TBX5, a member of the Brachyury (T) gene family. *Nat. Genet.* *15*, 21–29.
34. Rallis, C., Bruneau, B.G., Del Buono, J., Seidman, C.E., Seidman, J.G., Nissim, S., Tabin, C.J., and Logan, M.P.O. (2003). Tbx5 is required for forelimb bud formation and continued outgrowth. *Development* *130*, 2741–2751.
35. Bruneau, B.G., Nemer, G., Schmitt, J.P., Charron, F., Robitaille, L., Caron, S., Conner, D.A., Gessler, M., Nemer, M., Seidman, C.E., and Seidman, J.G. (2001). A murine model of Holt-Oram syndrome defines roles of the T-box transcription factor Tbx5 in cardiogenesis and disease. *Cell* *106*, 709–721.
36. Takeuchi, J.K., Koshiba-Takeuchi, K., Matsumoto, K., Vogel-Höpker, A., Naitoh-Matsuo, M., Ogura, K., Takahashi, N., Yasuda, K., and Ogura, T. (1999). Tbx5 and Tbx4 genes determine the wing/leg identity of limb buds. *Nature* *398*, 810–814.
37. Szenker-Ravi, E., Altunoglu, U., Leushacke, M., Bosso-Lefèvre, C., Khatoor, M., Thi Tran, H., Naert, T., Noelanders, R., Haja-mohideen, A., Beneteau, C., et al. (2018). RSPO2 inhibition of RNF43 and ZNRF3 governs limb development independently of LGR4/5/6. *Nature* *557*, 564–569.
38. Kircher, M., Witten, D.M., Jain, P., O’Roak, B.J., Cooper, G.M., and Shendure, J. (2014). A general framework for estimating the relative pathogenicity of human genetic variants. *Nat. Genet.* *46*, 310–315.
39. Naiche, L.A., and Papaioannou, V.E. (2007). Tbx4 is not required for hind limb identity or post-bud hind limb outgrowth. *Development* *134*, 93–103.
40. Vickerman, L., Neufeld, S., and Cobb, J. (2011). Shox2 function couples neural, muscular and skeletal development in the proximal forelimb. *Dev. Biol.* *350*, 323–336.
41. Arora, R., Metzger, R.J., and Papaioannou, V.E. (2012). Multiple roles and interactions of Tbx4 and Tbx5 in development of the respiratory system. *PLoS Genet.* *8*, e1002866.
42. Nimmakayalu, M., Major, H., Sheffield, V., Solomon, D.H., Smith, R.J., Patil, S.R., and Shchelochkov, O.A. (2011). Microdeletion of 17q22q23.2 encompassing TBX2 and TBX4 in a patient with congenital microcephaly, thyroid duct cyst, sensorineural hearing loss, and pulmonary hypertension. *Am. J. Med. Genet. A.* *155A*, 418–423.
43. Peterson, J.F., Ghaloul-Gonzalez, L., Madan-Khetarpal, S., Hartman, J., Surti, U., Rajkovic, A., and Yatsenko, S.A. (2014). Familial microduplication of 17q23.1–q23.2 involving TBX4 is associated with congenital clubfoot and reduced penetrance in females. *Am. J. Med. Genet. A.* *164A*, 364–369.
44. Schönewolf-Greulich, B., Ronan, A., Ravn, K., Baekgaard, P., Lodahl, M., Nielsen, K., Rendtorff, N.D., Tranøjgaard, L., Brøndum-Nielsen, K., and Tümer, Z. (2011). Two new cases with microdeletion of 17q23.2 suggest presence of a candidate gene for sensorineural hearing loss within this region. *Am. J. Med. Genet. A.* *155A*, 2964–2969.
45. Don, E.K., de Jong-Curtain, T.A., Doggett, K., Hall, T.E., Heng, B., Badrock, A.P., Winnick, C., Nicholson, G.A., Guillemin, G.J., Currie, P.D., et al. (2016). Genetic basis of hind limb loss in a naturally occurring vertebrate model. *Biol. Open* *5*, 359–366.
46. Lin, Q., Fan, S., Zhang, Y., Xu, M., Zhang, H., Yang, Y., Lee, A.P., Woltering, J.M., Ravi, V., Gunter, H.M., et al. (2016). The seahorse genome and the evolution of its specialized morphology. *Nature* *540*, 395–399.
47. Naert, T., Van Nieuwenhuysen, T., and Vleminckx, K. (2017). TALENs and CRISPR/Cas9 fuel genetically engineered clinically relevant *Xenopus tropicalis* tumor models. *Genesis* *55*, e23005.
48. Moreno-Mateos, M.A., Vejnar, C.E., Beaudoin, J.-D., Fernandez, J.P., Mis, E.K., Khokha, M.K., and Giraldez, A.J. (2015). CRISPRscan: Designing highly efficient sgRNAs for CRISPR-Cas9 targeting in vivo. *Nat. Methods* *12*, 982–988.
49. Boel, A., Steyaert, W., De Rocker, N., Menten, B., Callewaert, B., De Paepe, A., Coucke, P., and Willaert, A. (2016). BATCH-GE: Batch analysis of Next-Generation Sequencing data for genome editing assessment. *Sci. Rep.* *6*, 30330.



**Supplemental Data**

**Homozygous Null *TBX4* Mutations Lead to Posterior**

**Amelia with Pelvic and Pulmonary Hypoplasia**

**Ariana Kariminejad, Emmanuelle Szenker-Ravi, Caroline Lekszas, Homa Tajsharghi, Ali-Reza Moslemi, Thomas Naert, Hong Thi Tran, Fatemeh Ahangari, Minoo Rajaei, Mojila Nasser, Thomas Haaf, Afrooz Azad, Andrea Superti-Furga, Reza Maroofian, Siavash Ghaderi-Sohi, Hossein Najmabadi, Mohammad Reza Abbaszadegan, Kris Vleminckx, Pooneh Nikuei, and Bruno Reversade**

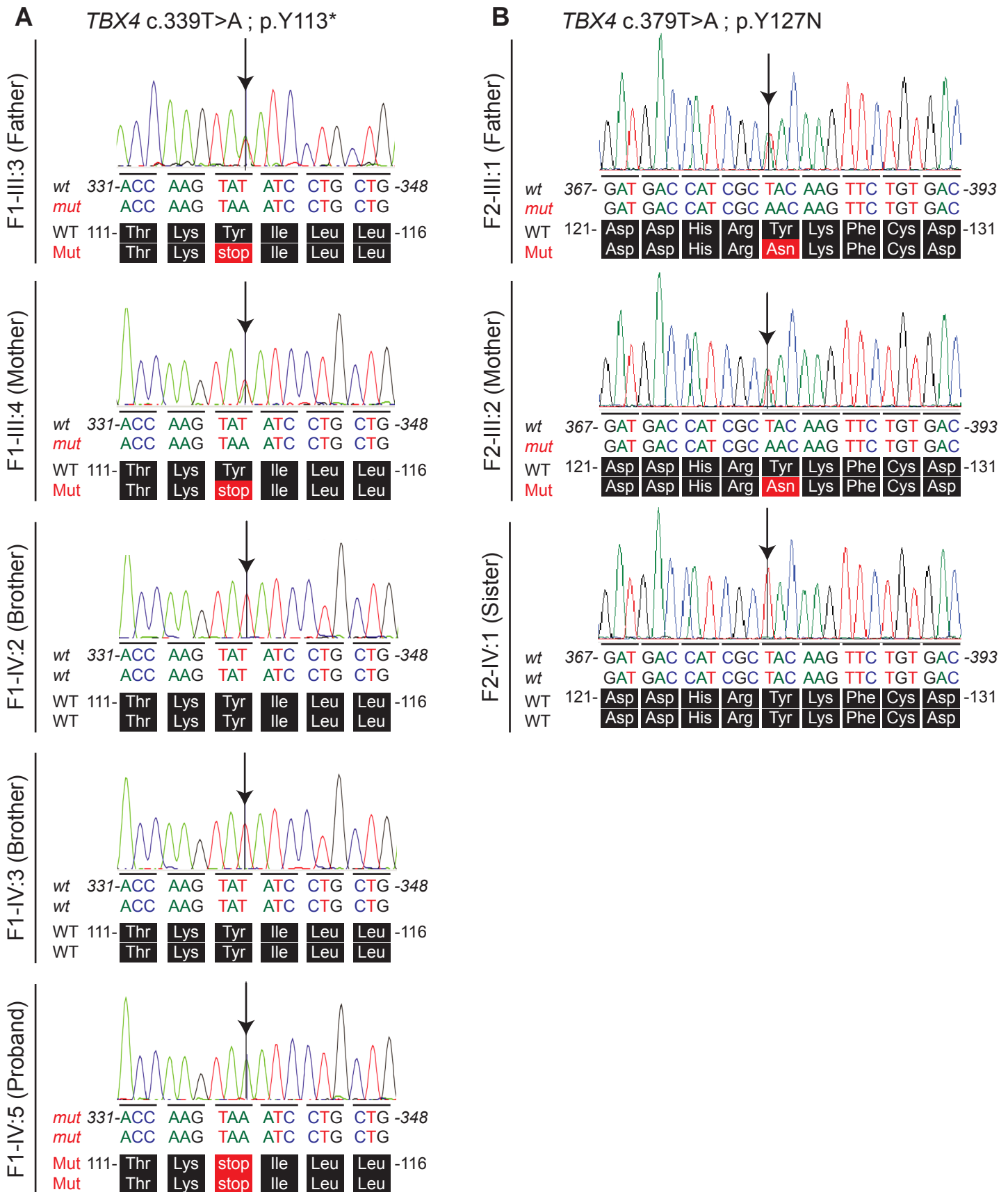


**Figure S1: Segregation analysis of causative germline *TBX4* mutations.** Sanger sequencing of *TBX4* mutations in available family members of Family 1 (a) and Family 2 (b). wt: wildtype, mut: mutant.

*Tbx4* crispant

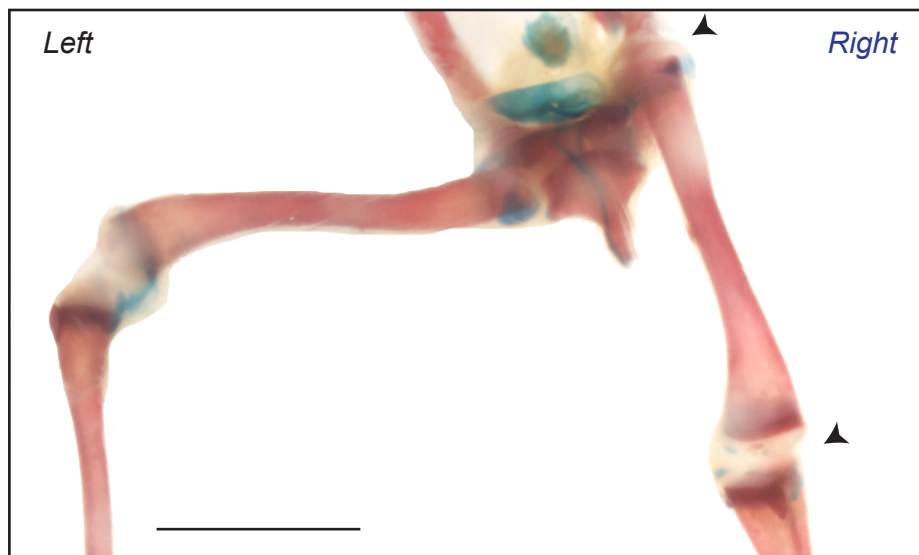
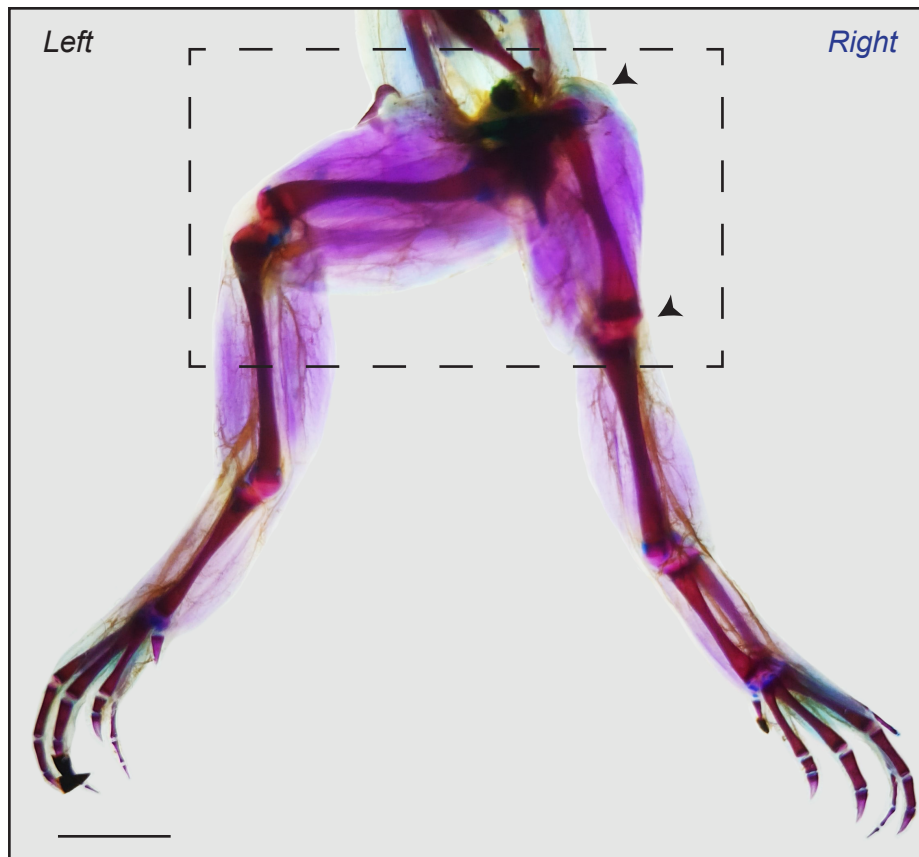


**Figure S2: Phenotype of mildly affected *Xenopus tropicalis* animals.** Representative images of an NF stage 66 adult animal, that had been unilaterally/ventrally injected with *Tbx4*\_gRNA2 and Cas9 protein at the 4-cell stage, stained with alizarin red/alcian blue. Note the dislocated joints (black arrowheads) both at the hip and knee, and the shorter femur of the hindlimb in the injected side (right). Scale bars: 0.2 cm.